(12 H, m), 1.72-2.10 (6 H, m), 3.16-4.44 (5 H, m), 4.99 (1 H, AB q, J = 12.6 Hz), 5.03 (1 H, AB q, J = 12.6 Hz), 7.33 (7 H, m).

(*S*)-(Benzyloxycarbonyl)-L-valyl-*N*-[1-acetyl-2-methylpropyl]-L-prolinamide (17). A solution of alcohol **16** (120 mg, 0.268 mmol) and 1-ethyl-3-[3-(dimethylamino)propyl]carbodiimide hydrochloride (514 mg, 2.68 mmol) in DMSO/toluene (1:1, 10 mL) was treated with dichloroacetic acid (0.090 mL, 1.1 mmol) and stirred for 16 h. The mixture was diluted with ethyl acetate, washed with 10% HCl and 10% HCl/brine (1:1), dried ($MgSO_4$), and evaporated. Purification by flash chromatography on silica gel, eluting with hexanes/acetone (4:1), gave **17** as a white solid (95 mg, 79%): TLC, R_f = 0.16, hexanes/acetone (4:1); HPLC, t_R = 8.98, FR = 2 mL/min, water/CH_3CN (3:2); MS (DCI) m/z = 446 (M + 1); ^1H NMR (DMSO-d_6) δ 0.97 (12 H, m), 1.70-2.20 (6 H, m), 2.06 (3 H, s), 3.58 (1 H, m), 3.71 (1 H, m), 4.07 (2 H, m), 4.44 (1 H, m), 4.99 (1 H, AB q, J = 12.6 Hz), 5.04 (1 H, AB q, J = 12.6 Hz), 7.35 (5 H, br s), 7.44 (1 H, d, J = 8.3 Hz), 8.07 (1 H, d, J = 8.0 Hz); Anal. ($C_{24}H_{35}N_3O_5$) C, H, N.

Kinetic Experiments. Kinetics of the inhibition of PPE or HLE by compounds **1-3**, **6**, **15**, and **17** were analyzed versus the synthetic substrate MeO-Suc-Ala-Ala-Pro-Val-pNA as discussed in the Kinetic Assay section of this paper. The inhibition constant of **18** was determined as previously reported.[8] HLE and PPE were obtained from Elastin Products and MeO-Suc-Ala-Ala-Pro-Val-pNA was purchased from Sigma. Progress curves were generated by recording the absorbance at 410 nm on a Cary 3 spectrophotometer for reaction solutions containing enzyme (7 nM HLE or 24 nM PPE), MeO-Suc-Ala-Ala-Pro-Val-pNA (160 μM for HLE, 500 μM for PPE), and several concentrations of inhibitor in either a pH 7.8 buffer (10 mM sodium phosphate, 500 mM NaCl) or pH 5.0 buffer (50 mM acetate, 500 mM NaCl) and 3.3% DMSO. Temperature was maintained at 25 °C with a Lauda K-RD circulating bath. Absorbances were continuously measured, digitized, and stored in a Compaq computer. Lineweaver-Burke plots were constructed from the reaction progress curves obtained as described above except that for the HLE assays the substrate concentration was varied between 25 and 600 μM, the inhibitor concentration was either zero or 15 nM, and the HLE concentration was 3 nM. For the PPE assays, the substrate concentration was varied between 0.125 and 1 mM, inhibitor concentration was either zero or 19 μM, and the PPE concentration was 48 nM.

Acknowledgment. We acknowledge the assistance of Dr. Charles Lerman and Dr. James Hall with the NMR experiments, Professor Robert Huber, MPIB, for the use of the FAST area detector, and support from the Robert A. Welch Foundation and The Texas Agricultural Experiment Station.

Synthesis and Structure Determination of the Adducts of the Potent Carcinogen 7,12-Dimethylbenz[*a*]anthracene and Deoxyribonucleosides Formed by Electrochemical Oxidation: Models for Metabolic Activation by One-Electron Oxidation

N. V. S RamaKrishna,[†] E. L. Cavalieri,*[,†] E. G. Rogan,[†] G. Dolnikowski,[‡] R. L. Cerny,[‡] M. L. Gross,[‡] H. Jeong,[§] R. Jankowiak,[§] and G. J. Small[§]

Contribution from the Eppley Institute for Research in Cancer, University of Nebraska Medical Center, 600 South 42nd Street, Omaha, Nebraska 68198-6805, Midwest Center for Mass Spectrometry, Department of Chemistry, University of Nebraska—Lincoln, Lincoln, Nebraska 68588, and Ames Laboratory-U.S. Department of Energy and Department of Chemistry, Iowa State University, Ames, Iowa 50011. *Received May 16, 1991*

Abstract: Anodic oxidation of 7,12-dimethylbenz[*a*]anthracene (7,12-DMBA) in the presence of dG yields four adducts and one oxygenated derivative of 7,12-DMBA: 7-methylbenz[*a*]anthracene (MBA)-12-CH_2-C8dG (13%), 7-MBA-12-CH_2-N7Gua (55%), 12-MBA-7-CH_2-N7Gua (12%), 7-MBA-12-CH_2-C8Gua (10%), and 7,12-$(CH_2OH)_2$-BA (10%). The first three are primary products of the electrochemical reaction, whereas the last two are secondary products. Binding occurs predominantly at the 12-CH_3 group of 7,12-DMBA and specifically to the N-7 and C-8 of Gua. On the other hand, anodic oxidation of 7,12-DMBA in the presence of dA gives only two detectable adducts: 7-MBA-12-CH_2-N7Ade (45%) and 12-MBA-7-CH_2-N3Ade (55%). Binding at the 12-CH_3 group is specific for the N-7 of Ade, whereas the 7-CH_3 group of 7,12-DMBA is specific for the N-3 of Ade. Structures of the adducts were elucidated by NMR and fast atom bombardment tandem mass spectrometry (FAB MS/MS). The adducts were also investigated by fluorescence line narrowing spectroscopy (FLNS). Both the FAB MS/MS and FLNS techniques can be used to distinguish between the adducts formed at the 7-CH_3 and 12-CH_3 groups of 7,12-DMBA (i.e., between 7-MBA-12-CH_2-N7Gua and 12-MBA-7-CH_2-N7Gua and between 7-MBA-12-CH_2-N7Gua and 7-MBA-12-CH_2-C8Gua). FLNS can distinguish 12-MBA-7-CH_2-N3Ade from 7-MBA-12-CH_2-N7Ade. On the other hand, the distinction between 7-MBA-12-CH_2-C8Gua and 7-MBA-12-CH_2-C8dG is straightforward by FAB MS but very difficult by FLNS. The electrochemical synthesis not only provides a demonstration of the specific reactivity of nucleosides and 7,12-DMBA under oxidizing conditions but is also a source of the necessary reference materials for studying the 7,12-DMBA-DNA adducts formed in biological systems. Furthermore, the analytical methodology is now appropriate for supporting in vivo studies of 7,12-DMBA-DNA adducts. A mechanism is proposed, although there are not sufficient data to prove it.

Introduction

Elucidation of the mechanisms of activation of polycyclic aromatic hydrocarbons (PAH) is central to an understanding of the process of tumor initiation and the design of preventive strategies. A powerful approach to this problem is to identify the structure of PAH-DNA adducts. Studies thus far point to two major mechanisms of activation: one-electron oxidation to form intermediate radical cations[1-4] and monooxygenation to produce

* Author to whom correspondence should be addressed.
† Eppley Institute for Research in Cancer.
‡ Midwest Center for Mass Spectrometry.
§ Iowa State University.

(1) Cavalieri, E.; Rogan, E. In *Free Radicals in Biology*; Pryor, W. A., Ed.; Academic: New York, 1984; Vol. VI, pp 323-369.

0002-7863/92/1514-1863$03.00/0

bay-region diol epoxides.[5,6] Hydroxylation of *meso*-anthracenic methyl groups followed by esterification can also represent an additional mechanism of carcinogenic activation for methylated PAH.[7-10]

Some evidence suggests that the bay-region diol epoxide of 7,12-dimethylbenz[*a*]anthracene (7,12-DMBA) is responsible for its carcinogenic activity. In fact, the only dihydrodiol potent in tumor initiation in mouse skin and induction of lung adenomas in newborn mice is 7,12-DMBA 3,4-dihydrodiol.[11,12] This proximate carcinogen is more potent than the parent 7,12-DMBA. A second line of evidence comes from analysis of 7,12-DMBA-DNA adducts. Three adducts have been identified as arising from addition of the bay-region diol epoxide of 7,12-DMBA to dA and dG.[13,14]

We propose that one-electron oxidation is a coherent mechanism of activation that can account for much of the carcinogenic activity of the most potent PAH, including benzo[*a*]pyrene (BP), 7,12-DMBA, and 3-methylcholanthrene. Common features of these PAH are (1) a relatively low ionization potential (IP) that allows metabolic removal of one electron with formation of a relatively stable radical cation and (2) appreciable charge localization in the PAH radical cation that renders this intermediate specifically and efficiently reactive toward nucleophiles.[1-4] Mammalian peroxidases, including prostaglandin H synthase,[15-18] and cytochrome P-450[19-24] catalyze one-electron oxidation, a mechanism involved not only in the formation of oxygenated metabolites[19,24] but also in the binding of PAH to DNA.[25-28] In the cytochrome P-450-catalyzed binding of BP to DNA, three major depurinated adducts have been identified (i.e., BP bound at C-6 to the C-8 of Gua, the N-7 of Gua, and the N-7 of Ade[28,29]). Furthermore, the depurinated adduct of BP bound at C-6 to the N-7 of Gua has been found in the urine of rats treated with BP,[30] and identification of other depurinated adducts formed in vivo is in progress. Fast atom bombardment tandem mass spectrometry (FAB MS/MS) and fluorescence line narrowing spectrometry (FLNS) have been essential in the identification of these adducts.[28-30]

The hypothesis for activation of 7,12-DMBA by one-electron oxidation comes from observations concerning the benz[*a*]-anthracene (BA) series, as well as the chemical properties of the 7,12-DMBA radical cation. The parent compound BA is a borderline carcinogen;[31] however, substitution of a methyl group at C-7 leads to substantially increased carcinogenicity.[32-34] Among the methyl-substituted BAs, the 7-CH_3 is the most active, followed by the 6-CH_3, 8-CH_3, and 12-CH_3 derivatives, whereas the others are inactive.[32-34] When two methyl groups are substituted at the meso-anthracenic positions of BA, the compound, 7,12-DMBA, becomes one of the most potent carcinogenic PAH.[31] Substitution of these two CH_3 with C_2H_5 groups renders the compound inactive.[35] The weak activity or inactivity of ethyl-substituted derivatives is a general phenomenon that has also been observed for 7-C_2H_5BA vs 7-CH_3BA[8] and for 6-C_2H_5BP vs 6-CH_3BP (unpublished results). Furthermore, 7-C_2H_5-12-CH_3BA exhibits the same carcinogenic activity as 7,12-DMBA, whereas 7-CH_3-12-C_2H_5BA is a much weaker carcinogen.[35] This may suggest that the 12-CH_3 group is involved in the critical activation of 7,12-DMBA.

One-electron oxidation of 7,12-DMBA by $Mn(OAc)_3$[3] or iodine–pyridine[36] produces nucleophilic substitution at the two CH_3 groups. For the latter oxidizing agent, the strong nucleophile pyridine also yields a 5-substituted pyridinium derivative. Nucleophilic substitution of the radical cation of a C_2H_5 PAH (for example, 7-C_2H_5BA) does not occur at the benzylic methylene because of stereoelectronic factors.[36] All of these observations point to the important role that CH_3 groups play in the carcinogenic activation of 7,12-DMBA.

Furthermore, 1,2,3,4-tetrahydro-7,12-DMBA, which is fully saturated in the angular ring and cannot be metabolically activated to the bay-region diol epoxide, is still a strong carcinogen.[37,38] Similarly, 1-F-7,12-DMBA and 4-F-7,12-DMBA, in which formation of the bay-region diol epoxide is blocked by the fluoro substituent, are also carcinogenic.[37-40] These results indicate that mechanisms other than formation of diol epoxides are involved in the carcinogenic activation of 7,12-DMBA.

To assess the importance of one-electron oxidation in the

(2) Cavalieri, E.; Rogan, E. In *Polycyclic Hydrocarbons and Carcinogenesis*; Harvey, R. G., Ed.; ACS Symposium Series 283; American Chemical Society: Washington, DC, 1985; pp 290–305.
(3) Cavalieri, E.; Rogan, E. *Environ. Health Perspect.* **1985**, *64*, 69–84.
(4) Cavalieri, E. L.; Rogan, E. G. *Free Radical Res. Commun.* **1990**, *11*, 77–87.
(5) Sims, P.; Grover, P. L. In *Polycyclic Hydrocarbons and Cancer*; Gelboin, H. V., Ts'o, P. O. P., Eds.; Academic: New York, 1981; pp 117–181.
(6) Conney, A. H. *Cancer Res.* **1982**, *42*, 4875–4917.
(7) Flesher, J. W.; Sydnor, K. L. *Int. J. Cancer* **1983**, *11*, 433–437.
(8) Cavalieri, E.; Roth, R.; Rogan, E. In *Polynuclear Aromatic Hydrocarbons*; Jones, P. W., Leber, P., Eds.; Ann Arbor Science: Ann Arbor, MI, 1979; pp 517–529.
(9) Rogan, E. G.; Cavalieri, E. L.; Walker, B. A.; Balasubramanian, R.; Wislocki, P. G.; Roth, R. W.; Saugier, R. K. *Chem.-Biol. Interact.* **1986**, *58*, 253–275.
(10) Surh, Y.-J.; Liem, A.; Miller, E. C.; Miller, J. A. *Carcinogenesis* **1989**, *10*, 1519–1528.
(11) Slaga, T. J.; Gleason, G. L.; DiGiovanni, J.; Sukumaran, K. B.; Harvey, R. G. *Cancer Res.* **1979**, *39*, 1934–1936.
(12) Wislocki, P. G.; Gadek, K. M.; Juliana, M. M.; MacDonald, J. S.; Chou, M. W.; Yang, S. K.; Lu, A. Y. H. In *Polynuclear Aromatic Hydrocarbons: Chemical Analysis and Biological Fate*; Cooke, M., Dennis, A. J., Eds.; Battelle Press: Columbus, OH, 1981; pp 675–685.
(13) Cheng, S. C.; Prakash, A. S.; Pigott, M. A.; Hilton, B. D.; Lee, H.; Harvey, R. G.; Dipple, A. *Carcinogenesis* **1988**, *9*, 1721–1723.
(14) Cheng, S. C.; Prakash, A. S.; Pigott, M. A.; Hilton, B. D.; Roman, J. M.; Lee, H.; Harvey, R. G.; Dipple, A. *Chem. Res. Toxicol.* **1988**, *1*, 216–221.
(15) Boyd, J. A.; Eling, T. E. *J. Biol. Chem.* **1984**, *22*, 13885–13896.
(16) Josephy, P. D.; Eling, T. E.; Mason, R. P. *J. Biol. Chem.* **1983**, *258*, 5561–5569.
(17) Degen, G. H.; Eling, T. E.; McLachlan, J. A. *Cancer Res.* **1982**, *42*, 919–923.
(18) Cavalieri, E.; Devanesan, P.; Rogan, E. *Biochem. Pharmacol.* **1988**, *37*, 2183–2188.
(19) Cavalieri, E.; Rogan, E.; Cremonesi, P.; Devanesan, P. *Biochem. Pharmacol.* **1988**, *37*, 2173–2182.
(20) Hanzlik, R. P.; Tullman, R. H. *J. Am. Chem. Soc.* **1982**, *104*, 2048–2050.
(21) MacDonald, T. L.; Zirvi, K.; Burka, L. T.; Peyman, P.; Guengerich, F. P. *J. Am. Chem. Soc.* **1982**, *104*, 2050–2052.
(22) Augusto, O.; Beilan, H. S.; Ortiz de Montellano, P. R. *J. Biol. Chem.* **1982**, *257*, 11288–11295.
(23) Burka, L. T.; Guengerich, F. P.; Willard, R. J.; MacDonald, T. L. *J. Am. Chem. Soc.* **1985**, *107*, 2549–2551.
(24) Stearns, R. A.; Ortiz de Montellano, P. R. *J. Am. Chem. Soc.* **1985**, *107*, 4081–4082.
(25) Cavalieri, E. L.; Rogan, E. G.; Roth, R. W.; Saugier, R. K.; Hakam, A. *Chem.-Biol. Interact.* **1983**, *47*, 87–109.
(26) Devanesan, P.; Rogan, E.; Cavalieri, E. *Chem.-Biol. Interact.* **1987**, *61*, 89–95.
(27) Rogan, E.; Cavalieri, E.; Tibbels, S.; Cremonesi, P.; Warner, C.; Nagel, D.; Tomer, K.; Cerny, R.; Gross, M. *J. Am. Chem. Soc.* **1988**, *110*, 4023–4029.
(28) Cavalieri, E. L.; Rogan, E. G.; Devanesan, P. P.; Cremonesi, P.; Cerny, R. L.; Gross, M. L.; Bodell, W. J. *Biochemistry* **1990**, *29*, 4820–4827.
(29) Devanesan, P. D.; RamaKrishna, N. V. S.; Todorovic, R.; Rogan, E. G.; Cavalieri, E. L.; Jeong, H.; Jankowiak, R.; Small, G. J. *Chem. Res. Toxicol.* **1992**, in press.
(30) Rogan, E. G.; RamaKrishna, N. V. S.; Higginbotham, S.; Cavalieri, E. L.; Jeong, H.; Jankowiak, R.; Small, G. J. *Chem. Res. Toxicol.* **1990**, *3*, 441–444.
(31) Dipple, A. In *Chemical Carcinogens*; Searle, C. E., Ed.; American Chemical Society: Washington, DC, 1976; pp 245–314.
(32) Dunning, W. F.; Curtis, M. P. *J. Natl. Cancer Inst.* **1960**, *25*, 387–391.
(33) Stevenson, J. L.; VanHamm, E. *Am. Inst. Hyg. Assoc. J.* **1965**, *26*, 475–478.
(34) Wislocki, P. G.; Fiorentin, K. M.; Fu, P. P.; Yang, S. K.; Lu, A. Y. H. *Carcinogenesis* **1982**, *3*, 215–217.
(35) Pataki, J.; Balick, R. *J. Med. Chem.* **1972**, *15*, 905–909.
(36) Cavalieri, E.; Roth, R. *J. Org. Chem.* **1976**, *41*, 2679–2684.
(37) DiGiovanni, J.; Diamond, L.; Singer, J. M.; Daniel, F. B.; Witiak, D. T.; Slaga, T. J. *Carcinogenesis* **1982**, *3*, 651–655.
(38) Cavalieri, E. L.; Rogan, E. G.; Higginbotham, S.; Cremonesi, P.; Salmasi, S. *Polycyclic Aromat. Compd.* **1990**, *1*, 59–70.
(39) Harvey, R. G.; Dunne, F. B. *Nature (London)* **1978**, *273*, 566–568.
(40) DiGiovanni, J.; Decina, P. C.; Diamond, L. *Carcinogenesis* **1983**, *4*, 1045–1049.

metabolic activation of 7,12-DMBA, nucleoside adducts must be synthesized, isolated, and identified. Synthesis of deoxyribonucleoside adducts by electrochemical oxidation of 7,12-DMBA serves several purposes: (1) to confirm the selective reactivity of the CH_3 groups in the 7,12-DMBA radical cation, (2) to determine the nucleophilic groups in the nucleic acid bases that participate in adduct formation, (3) to prepare standards for identifying and quantifying these adducts in biological systems, and (4) to provide evidence for a mechanism of adduct formation.

We report in this paper the results of anodic oxidation of 7,12-DMBA in the presence of dG or dA and determination of the structure of the resulting adducts by NMR, FAB MS/MS, and FLNS. A mechanism for the reaction of 7,12-DMBA with deoxyribonucleosides is proposed, although insufficient data are available to prove it.

Experimental Section

General Procedures. UV absorbance spectra were recorded with a Waters 990 photodiode array (PDA) detector during high-pressure liquid chromatography (HPLC) with a CH_3OH/H_2O gradient.

a. NMR. Proton and homonuclear two-dimensional chemical shift correlation spectroscopy (COSY) and nuclear Overhauser effect (NOE) NMR spectra were recorded on a Varian XL-300 instrument at 299.938 MHz in DMSO-d_6 at 30 °C. Chemical shifts (δ) are reported relative to tetramethylsilane, which was employed either as a primary internal reference or as a secondary reference relative to DMSO at 2.50 ppm, and the J values are given in hertz. Typical instrument parameters were as previously reported.[27]

NOE difference spectra were recorded by applying a presaturation pulse with a decoupler on resonance and subtracting the trace from the corresponding reference spectra recorded under identical conditions but with the decoupler off-resonance. Typical spectra were obtained from at least 2560 transients.

b. FAB MS/MS. Mass spectrometry experiments were performed either on a Kratos MS-50 triple-analyzer tandem mass spectrometer with an E_1BE_2 geometry[41] or on a prototype ZAT-T, a four-sector tandem instrument of $B_1E_1B_2E_2$ geometry. A description of the ZAB-T will be published separately. The adducts were ionized either by argon fast atom bombardment (triple-analyzer) or by Cs^+ secondary ion mass spectrometry (four-sector) from a 5:1 dithiothreitol/dithioerythritol (DTT/DTE) matrix. Other matrix materials such as glycerol and 3-nitrobenzyl alcohol were tried, but DTT/DTE provided the best sample ion current. Collisional activation decompositions (CAD) were initiated with helium in a grounded collision cell. The parent ions were selected by the first electrostatic analyzer and the magnet with a resolving power of 2000 to remove interference from isobaric matrix ions. On the Kratos MS-50 triple-analyzer, collision-induced dissociation daughter ion mass spectra were collected by scanning the second electrostatic analyzer and detected with an electron multiplier equipped with postacceleration dynode. Data were collected and processed by using a Data General Nova/4 computer operated with custom software. MS/MS spectra were acquired on the ZAB-T in a B_2/E_2 linked scan mode. Data were collected in a multichannel analyzer mode by using the VG OPUS operating system and a VAX 3100 work-station.

c. FLNS. The FLNS apparatus utilized for the present studies was previously described in detail.[42,43] Briefly, the excitation laser was a Lambda Physik FL-2002 dye laser pumped by a Lambda Physik EMG 102 MSC excimer (XeCl gas) laser. The laser pulse width was 10 ns. Fluorescence was dispersed by a McPherson 2061 monochromator, which has a reciprocal linear dispersion of 0.42 nm/mm, and detected with a Princeton Instruments IRY-1022/G/R/B intensified blue-enhanced PDA. The spectral resolution was limited by the PDA to 3 cm^{-1} at 400 nm. With the above monochromator, the PDA provided a ca. 9-nm segment of the fluorescence spectrum for a given monochromator setting. The detection electronics provided for a gating time as short as 5 ns. For reasons discussed below, a gate delay time of 50 ns with an observation window of 60 ns was employed. The glass-forming solvent utilized was (by volume) 50% glycerol, 40% H_2O, and 10% ethanol. Adducts were first dissolved in about 10 μL of DMSO at concentrations of 10^{-7}–10^{-8} M and subsequently mixed with ca. 30 μL of the glass solvent. Quartz tubes (3 mm o.d. × 2 mm i.d. × 1 cm) were used to contain the solutions (ca. 40 μL total volume). Samples were rapidly cooled (ca. 2 min) in a double-nested glass liquid helium Dewar equipped with fused quartz optical windows. All FLN spectra reported here were obtained with the laser excitation frequency tuned to vibronic absorption regions of the $S_1 \leftarrow S_0$ absorption system and are referred to as vibronically excited FLN spectra.[42-44]

d. HPLC. HPLC was conducted on a Waters 600E solvent delivery system equipped with a Waters 700 WISP autoinjector. Effluents were monitored for UV absorbance (254 nm) with a Waters 990 PDA detector, and the data were collected on an APC-IV Powermate computer. Analytical runs were conducted on a YMC (YMC, Overland Park, KS) ODS-AQ 5 μm column (6.0 × 250 mm). After the column was eluted for 5 min with 30% CH_3CN in H_2O, a 70-min curvilinear gradient (CV7) to 100% CH_3CN was run at 1 mL/min. Preparative HPLC was conducted on a YMC ODS-AQ 5 μm, 120 Å column (20 × 250 mm) at a flow rate of 6 mL/min with the above gradient.

Electrochemical Synthesis of Adducts. Electrochemical synthesis was conducted with an apparatus (EG&G Princeton Applied Research, Princeton, NJ) as previously described.[27] The electrolysis potential for 7,12-DMBA was 1.198 V, that is the anodic peak potential measured in DMF by cyclic voltammetry with a Nicolet 310 digital oscilloscope (Test Instruments Division, Madison, WI) coupled with a Model 175 universal programmer and Model 179 digital coulometer (EG&G Princeton Applied Research, Princeton, NJ). The cyclic voltammetry of 7,12-DMBA in DMF under reversible conditions revealed that oxidation of this compound involves only one electron (unpublished results). The potential used for the synthesis of 7,12-DMBA adducts was 1.10 V, which is slightly less than its anodic peak potential. The cyclic voltammetry of individual deoxyribonucleosides was also performed in DMF. The anodic peak potential of dG was determined to be 1.31 V. The anodic peak potentials of dA, dC, and T could not be determined in DMF because this solvent began to be oxidized at 1.45 V, indicating that the anodic potentials of dA, dC, and T are above this value. Thus, during adduct synthesis at 1.10 V, none of the nucleosides, including dG, was oxidized. To confirm this, four different electrochemical reactions were conducted with 7,12-DMBA/dG molar ratios of 1:2.5, 1:5.0, 1:7.5, and 1:10, and the products were analyzed by HPLC. The relative ratios of the adducts in all four reactions were similar, but the best conversion of 7,12-DMBA to adducts was achieved at a molar ratio of 1:10. Hence, the 7,12-DMBA-dG adduct preparations were conducted at this molar ratio.

Commercially available DMF (Aldrich) was purified by refluxing over CaH_2, followed by vacuum distillation just prior to use, and was stored over 4-Å molecular sieves under argon. $KClO_4$ (Aldrich) was used as obtained. 7,12-DMBA was purified by column chromatography on silica gel by eluting with benzene/hexane (1:1). The product was recrystallized from benzene/methanol (mp 121–122 °C). The nucleosides dG, dA, dC, and T (Pharmacia P-L Biochemicals, Piscataway, NJ) were desiccated over P_2O_5 under vacuum at 110 °C for 48 h prior to use. The 7-methylbenz[a]anthracene (MBA)-12-CH_2Br, 7-MBA-12-CH_2OAc, 12-MBA-7-CH_2Br, and 12-MBA-7-CH_2OAc were prepared according to published procedures.[36]

All glassware, syringes, needles, electrochemical cell, and platinum working and reference electrodes were oven-dried at 150 °C prior to use. The electrochemical cell and working electrode were assembled while hot and then cooled under argon.

Coupling between 7,12-DMBA and nucleophilic groups of deoxyribonucleosides was accomplished by selective anodic oxidation of the PAH in the presence of the nucleoside. In a typical preparation, DMF (35 mL) containing 0.5 M $KClO_4$ as the supporting electrolyte was pre-electrolyzed at +1.45 V, while argon was bubbled into the cell, until no appreciable current could be detected (ca. 30 min). The nucleoside (389 μmol) was added, and stirring was continued until the solution was clear. Bubbling of argon was stopped and a positive pressure was maintained. 7,12-DMBA (39 μmol) was added as a solid; when it was dissolved, the cell was switched on, and the electrode potential was gradually raised from 0 to 1.10 V and kept constant at this value during the entire electrolysis. Both the output current (i) and the total charge (Q) were monitored throughout the experiment. The reaction was stopped when i had decreased to ca. $^1/_{20}$ of the initial value and a charge twice the theoretical charge expected (for a two-electron transfer) had accumulated. These two conditions were usually achieved in ca. 90 min.

After the reaction was complete, DMF was removed under vacuum, the adducts were extracted four times from the solid ($KClO_4$) by using a solvent mixture of ethanol/chloroform/acetone (2:1:1), and the resulting extract was filtered through a Whatman fluted filter paper. The combined solvent mixture was evaporated under vacuum, and the residue was dissolved in 3 mL of DMSO, filtered through a 0.45-μm filter, and

(41) Gross, M. L.; Chess, E. K.; Lyon, P. A.; Crow, F. W.; Evans, S.; Tudge, H. *Int. J. Mass Spectrom. Ion Phys.* **1982**, *42*, 243–254.
(42) Jankowiak, R.; Small, G. J. *Anal. Chem.* **1989**, *61*, 1023–1032.
(43) Lu, P.; Jeong, H.; Jankowiak, R.; Small, G. J.; Kim, S. K.; Cosman, M.; Geacintov, N. E. *Chem. Res. Toxicol.* **1991**, *4*, 58–69.
(44) Zamzow, D.; Jankowiak, R.; Cooper, R. S.; Small, G. J.; Tibbels, S. R.; Cremonesi, P.; Devanesan, P.; Rogan, E. G.; Cavalieri, E. L. *Chem. Res. Toxicol.* **1989**, *2*, 29–34.

Scheme I. Electrochemical Oxidation of 7,12-DMBA in the Presence of dG or dA

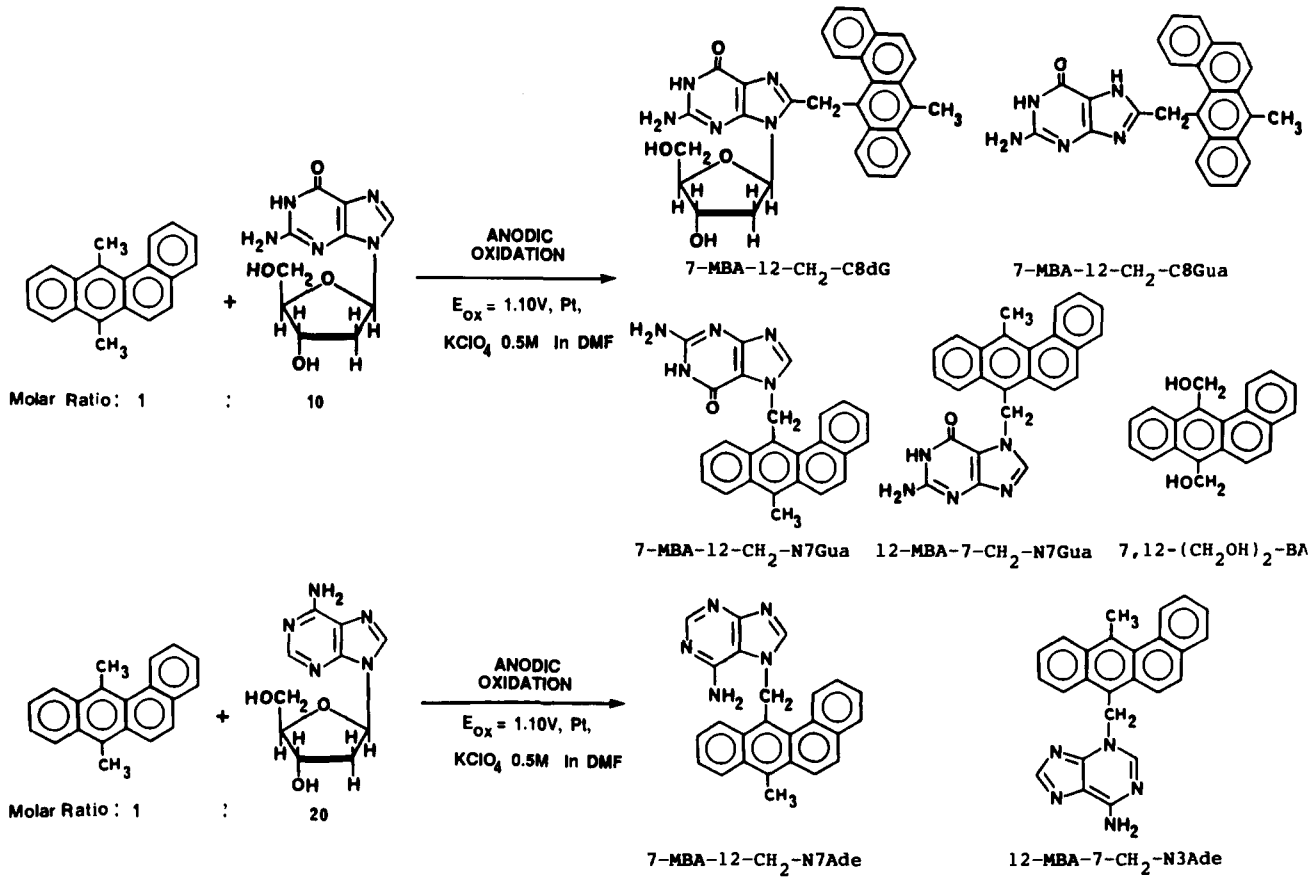

analyzed by HPLC with the CH_3CN/H_2O gradient. Purification of the adducts was conducted by preparative HPLC in CH_3CN/H_2O, followed by the CH_3OH/H_2O gradient.

The isolated products from the 7,12-DMBA and dG reaction were 7-MBA-12-CH_2-C8dG (13%), 7,12-$(CH_2OH)_2$-BA (10%), 7-MBA-12-CH_2-C8Gua (10%), 7-MBA-12-CH_2-N7Gua (55%), and 12-MBA-7-CH_2-N7Gua (12%) (Scheme I). The reaction between 7,12-DMBA and dA gave two products: 7-MBA-12-CH_2-N7Ade (45%) and 12-MBA-7-CH_2-N3Ade (55%) (Scheme I). The reaction between 7,12-DMBA and dC or T resulted in no detectable products.

a, 7,12-DMBA, UV λ_{max} (nm) 236, 264, 286, 296, 365, 384; NMR 3.01 (s, 3 H, 7-CH_3), 3.26 (s, 3 H, 12-CH_3), 7.60 (m, 2 H, 2-H, 3-H), 7.66 (m, 3 H, 5-H, 9-H, 10-H), 7.90 (d, 1 H, 4-H), 8.05 (d, 1 H, 6-H), 8.38 (m, 2 H, 8-H, 11-H), 8.49 (d, 1 H, 1-H).

b, 7-MBA-12-CH_2-C8dG, UV λ_{max} (nm) 224, 250, 294, 304, 368, 384; NMR 2.11 (m, 1 H, 2′-H), 2.65 (m, 1 H, 2′-H), 3.05 (s, 3 H, 7-CH_3), 3.43 (m, 2 H, 5′-H_2), 3.68 (m, 1 H, 4′-H), 4.26 (m, 1 H, 3′-H), 4.90 (bs, 1 H, 5′-OH), 5.09 (bs, 1 H, 3′-OH), 5.19 (s, 2 H, 12-CH_2), 6.10 (t, 1 H, 1′-H), 7.48 (t, 1 H, 3-H), 7.53 (t, 1 H, 2-H), 7.59–7.75 (m, 5 H, 5-H, 9-H, 10-H, 2-NH_2[Gua]), 7.88 (d, 1 H, 4-H), 8.09 (d, 1 H, 6-H), 8.29 (d, 1 H, 11-H), 8.41 (d, 1 H, 8-H), 8.59 (d, 1 H, 1-H).

c, 7-MBA-12-CH_2-C8Gua, UV λ_{max} (nm) 224, 274, 294, 304, 374, 384; NMR 3.08 (s, 3 H, 7-CH_3), 5.21 (s, 2 H, 12-CH_2), 6.73 (bs, 1 H, 7- or 9-NH[Gua]), 7.56 (t, 1 H, 3-H), 7.61 (t, 1 H, 2-H), 7.65–7.80 (m, 5 H, 5-H, 9-H, 10-H, 2-NH_2[Gua]), 7.95 (d, 1 H, 4-H), 8.14 (d, 1 H, 6-H), 8.30 (d, 1 H, 11-H), 8.46 (d, 1 H, 8-H), 8.53 (d, 1 H, 1-H).

d, 7-MBA-12-CH_2-N7Gua, UV λ_{max} (nm) 228, 276, 296, 306, 372, 384; NMR 3.14 (s, 3 H, 7-CH_3), 6.32 (s, 2 H, 12-CH_2), 7.20 (bs, 2 H, 2-NH_2[Gua]), 7.48 (t, 1 H, 3-H), 7.61–7.72 (m, 3 H, 9-H, 10-H, 2-H), 7.76 (d, 1 H, 5-H), 7.91–8.04 (m, 3 H, 11-H, 4-H, 1-H), 8.20 (d, 1 H, 6-H), 8.26 (s, 1 H, 8-H[Gua]), 8.49 (d, 1 H, 8-H).

e, 12-MBA-7-CH_2-N7Gua, UV λ_{max} (nm) 228, 274, 294, 304, 372, 384; NMR 3.20 (s, 3 H, 12-CH_3), 5.36 (s, 2 H, 7-CH_2), 6.09 (bs, 1 H, 2-NH_2[Gua]), 6.41 (s, 1 H, 2-NH_2[Gua]), 6.85 (s, 1 H, 8-H[Gua]), 7.51–7.71 (m, 4 H, 2-H, 3-H, 9-H, 10-H), 7.73–7.85 (m, 2 H, 4-H, 5-H), 8.11 (d, 1 H, 6-H), 8.31 (d, 1 H, 8-H), 8.41 (m, 2 H, 1-H, 11-H).

f. 7,12-$(CH_2OH)_2$-BA, UV λ_{max} (nm) 236, 264, 286, 296, 365, 384; NMR 5.30 (s, 2 H, 7-CH_2), 5.45 (s, 2 H, 12-CH_2), 6.0 (bs, 2 H, 7-OH, 12-OH), 7.62–7.75 (m, 5 H, 2-H, 3-H, 5-H, 9-H, 10-H), 7.95 (d, 1 H, 4-H), 8.23 (d, 1 H, 6-H), 8.50 (d, 1 H, 11-H), 8.65 (d, 1 H, 8-H), 9.05 (d, 1 H, 1-H).

g, 7-MBA-12-CH_2-N7Ade, UV λ_{max} (nm) 216, 286, 294, 362, 400; NMR 3.17 (s, 3 H, 7-CH_3), 6.46 (s, 2 H, 12-CH_2), 7.16 (bs, 2 H, 6-NH_2[Ade]), 7.42 (t, 1 H, 3-H), 7.59–7.72 (m, 4 H, 2-H, 8-H[Ade], 9-H, 10-H), 7.74–7.88 (m, 2 H, 1-H, 5-H), 7.96–8.05 (m, 2 H, 4-H, 11-H), 8.23 (d, 1 H, 6-H), 8.29 (s, 1 H, 2-H[Ade]), 8.54 (d, 1 H, 8-H).

h, 12-MBA-7-CH_2-N3Ade, UV λ_{max} (nm) 220, 286, 294, 362, 384; NMR 3.39 (s, 3 H, 12-CH_3), 6.52 (s, 2 H, 7-CH_2), 6.98 (s, 1 H, 2-H-[Ade]), 7.27 (bs, 2 H, 6-NH_2[Ade]), 7.58–7.78 (m, 5 H, 2-H, 3-H, 5-H, 9-H, 10-H), 7.93 (m, 1 H, 4-H), 8.02 (d, 1 H, 6-H), 8.24 (s, 1 H, 8-H[Ade]), 8.29 (d, 1 H, 8-H), 8.48 (d, 1 H, 11-H), 8.56 (m, 1 H, 1-H).

Reaction of 12-MBA-7-CH_2Br and dG. A mixture of 5 mg (14.9 μmol) of 12-MBA-7-CH_2Br and 50 mg (187.2 μmol) of dG was dissolved in 10 mL of dry DMF and stirred at room temperature for 24 h under anhydrous conditions. Analysis of an aliquot by HPLC in CH_3CN/H_2O showed the complete disappearance of starting material and presence of two peaks with retention times of 53.9 (52%) and 59.4 min (48%). Both compounds were purified by preparative HPLC, and their structures were established by NMR and FAB MS. The peak with retention time of 53.9 min corresponds to 12-MBA-7-CH_2-N^2dG, and the peak at 59.4 min corresponds to 12-MBA-7-CH_2-N7Gua.

a, 12-MBA-7-CH_2N^2dG, UV λ_{max} (nm) 220, 286, 294, 362, 384; NMR 2.34 (m, 1 H, 2′-H), 2.71 (m, 1 H, 2′-H), 3.16 (s, 3 H, 12-CH_3), 3.60 (m, 2 H, 5′-H_2), 3.89 (m, 1 H, 4′-H), 4.44 (m, 1 H, 3′-H), 4.92 (bs, 1 H, 5′-OH), 5.34 (bs, 1 H, 3′-OH), 5.41 (s, 2 H, 7-CH_2), 6.37 (t, 1 H, 1′-H), 7.56–7.79 (m, 6 H, 5-H, 9-H, 10-H, 2-H, 3-H, 2-NH[Gua]), 7.89 (m, 1 H, 4-H), 7.95 (s, 1 H, 8-H[Gua]), 8.22 (d, 1 H, 6-H), 8.39 (m, 1 H, 8-H), 8.43–8.56 (m, 2 H, 1-H, 11-H); MS $(M + H)^+$ of m/z 522.2168; theoretical mass of $C_{30}H_{28}N_5O_4$ 522.2141.

b, 12-MBA-7-CH_2-N7Gua, UV λ_{max} (nm) 228, 274, 294, 304, 372, 384; NMR 3.20 (s, 3 H, 12-CH_3), 5.36 (s, 2 H, 7-CH_2), 6.09 (bs, 1 H, 2-NH_2[Gua]), 6.41 (s, 1 H, 2-NH_2[Gua]), 6.85 (s, 1 H, 8-H[Gua]), 7.51–7.71 (m, 4 H, 2-H, 3-H, 9-H, 10-H), 7.73–7.85 (m, 2 H, 4-H, 5-H), 8.11 (d, 1 H, 6-H), 8.31 (d, 1 H, 8-H), 8.41 (m, 2 H, 1-H, 11-H); MS $(M + H)^+$ of m/z 406.1647; theoretical mass of $C_{25}H_{26}N_5O$ 406.1667.

Reaction of 7-MBA-12-CH_2OAc and dG. A mixture of 5 mg of 7-MBA-12-CH_2OAc (15.9 μmol) and 50 mg (187.2 μmol) of dG was dissolved in 10 mL of dry DMF and stirred at room temperature for 24 h under anhydrous conditions. No reaction was detected. The mixture was heated at 90 °C for 6 h; no reaction was detected. The mixture was then heated at 140 °C. After 10 h, the reaction was complete, and a product with retention time of 57.4 min on HPLC (91%) was observed.

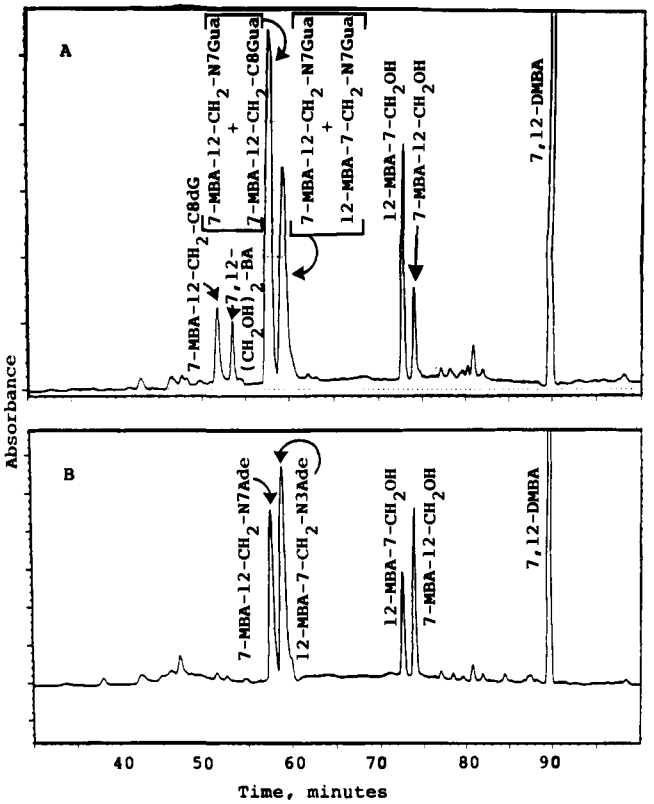

Figure 1. HPLC separation of the products obtained by electrochemical oxidation of 7,12-DMBA in the presence of (A) dG or (B) dA.

After purification by preparative HPLC, this product was identified as 7-MBA-12-CH_2-N^2Gua.

a, 7-MBA-12-CH_2-N^2Gua. UV λ_{max} (nm) 228, 276, 296, 306, 372, 384; NMR 3.15 (s, 3 H, 7-CH_3), 6.30 (s, 2 H, 12-CH_2), 6.45 (bs, 1 H, NH[Gua]), 7.17 (s, 1 H, NH[Gua]), 7.47 (t, 1 H, 3-H), 7.59–7.71 (m, 3 H, 9-H, 10-H, 2-H), 7.84 (d, 1 H, 5-H), 7.90–8.01 (m, 3 H, 11-H, 4-H, 1-H), 8.21 (d, 1 H, 6-H), 8.30 (s, 1 H, 8-H[Gua]), 8.50 (d, 1 H, 8-H); MS $(M + H)^+$ of m/z 406.1693; theoretical mass of $C_{25}H_{26}N_5O$ 406.1667.

Reaction of 7-MBA-12-CH_2Br and dG. The same reaction conditions were used as above except that the reaction was carried out at 140 °C for 24 h. Only one product was obtained, in 15% yield. The yield was not increased when the reaction was continued for an additional 48 h at 140 °C. The purified product was confirmed to be 7-MBA-12-CH_2-N^2Gua by NMR, and the empirical formula was confirmed by high-resolution MS.

Reaction of 12-MBA-7-CH_2OAc and dG. The same reaction conditions were employed as with 7-MBA-12-CH_2OAc. No reaction was detected. When the reaction was conducted for an additional 24 h at 140 °C, less than 1% product formation was detected.

Results and Discussion

Synthesis of Adducts by Electrochemical Oxidation. Anodic oxidation of 7,12-DMBA in the presence of dG consistently yielded four adducts and one oxygenated derivative of 7,12-DMBA: 7-MBA-12-CH_2-C8dG (13%), 7-MBA-12-CH_2-C8Gua (10%), 7-MBA-12-CH_2-N7Gua (55%), 12-MBA-7-CH_2-N7Gua (12%), and 7,12-$(CH_2OH)_2$-BA (10%) (Scheme I). Adducts were separated and purified by HPLC (Figure 1A). Among the five products, three adducts, 7-MBA-12-CH_2C8dG, 7-MBA-12-CH_2-N7Gua, and 12-MBA-7-CH_2-N7Gua, are the primary products; the two secondary products, 7-MBA-12-CH_2-C8Gua and 7,12-$(CH_2OH)_2$-BA, are formed from further anodic oxidation of 7-MBA-12-CH_2C8dG and 12-MBA-7-CH_2-N7Gua, respectively.

Approximately 40% of the 7-MBA-12-CH_2-C8dG formed lost the deoxyribose moiety to yield 7-MBA-12-CH_2-C8Gua. In the HPLC separation with the CH_3CN/H_2O curvilinear gradient, 7-MBA-12-CH_2-C8dG eluted at 51.3 min and 7,12-$(CH_2OH)_2$-BA at 54.0 min. 7-MBA-12-CH_2-C8Gua eluted at 56 min together with 7-MBA-12-CH_2-N7Gua. In addition, a portion of the 7-MBA-12-CH_2-N7Gua also eluted with 12-MBA-7-CH_2-N7Gua. The 7-MBA-12-CH_2-C8Gua and 7-MBA-12-CH_2-N7Gua were then separated and purified with a second gradient of 60% CH_3OH in H_2O for 5 min, followed by a 40-min linear gradient to 100% CH_3OH at a flow rate of 4 mL/min. Similarly, the 12-MBA-7-CH_2-N7Gua and 7-MBA-12-CH_2-N7Gua were separated by conducting preparative HPLC in 50% CH_3CN in H_2O for 5 min followed by a 50-min linear gradient to 100% CH_3CN at a flow rate of 4 mL/min.

To demonstrate the pathway by which the secondary adduct 7-MBA-12-CH_2-C8Gua is formed, 7-MBA-12-CH_2-C8dG was electrochemically oxidized under the conditions in which the adducts were prepared. After nearly 90 min of reaction, the products were analyzed by HPLC. The analysis showed that 37% of 7-MBA-12-CH_2-C8dG lost the sugar to form 7-MBA-12-CH_2-C8Gua.

To prove how the secondary product 7,12-$(CH_2OH)_2$-BA is formed, each of the two N7Gua adducts, 7-MBA-12-CH_2-N7Gua and 12-MBA-7-CH_2-N7Gua, was electrochemically oxidized in the presence of a 10-fold excess of dG under the conditions in which the adducts were prepared. The products were analyzed by HPLC in the two different solvent systems, CH_3CN/H_2O and CH_3OH/H_2O. HPLC analysis shows that the 7,12-$(CH_2OH)_2$-BA is formed only by oxidation of 12-MBA-7-CH_2-N7Gua, whereas 7-MBA-12-CH_2-N7Gua does not react. The formation of 7,12-$(CH_2OH)_2$-BA probably begins with oxidation of 12-MBA-7-CH_2-N7Gua and reaction of the N-7 of dG with the 12-CH_3 group. An N7Gua diadduct is apparently formed and is easily hydrolyzed to 7,12-$(CH_2OH)_2$-BA during HPLC.

When the reaction between 7,12-DMBA and dA was conducted at a molar ratio of 1:10, no appreciable amounts of adducts were formed. The reaction was successfully carried out, however, at a molar ratio of 7,12-DMBA to dA equal to 1:20. This afforded two adducts: 7-MBA-12-CH_2-N7Ade (45%) and 12-MBA-7-CH_2-N3Ade (55%) (Scheme I and Figure 1B). With the CH_3CN/H_2O curvilinear gradient, 7-MBA-12-CH_2-N7Ade eluted at 57.7 min and 12-MBA-7-CH_2-N3Ade at 59.0 min. These two adducts were purified by conducting preparative HPLC in 30% CH_3CN in H_2O at 6 mL/min for 5 min, followed by the curvilinear gradient to 100% CH_3CN in 75 min. Finally, the purity of all of the adducts was independently checked by HPLC in the two solvent systems, CH_3CN/H_2O and CH_3OH/H_2O.

The reactions of 7,12-DMBA with dC and T were performed at both 1:10 and 1:20 molar ratios. HPLC analysis indicated no detectable formation of adducts.

The UV spectra of the adducts are nearly the same as that of 7,12-DMBA because the covalent bond of the nucleic acid moieties is at one of the methyl groups and does not produce any appreciable conjugation with the aromatic rings of the 7,12-DMBA moiety.

Structure Elucidation by NMR. The structures of the synthesized adducts were elucidated by using proton NMR, with the support of COSY and NOE spectra.

a, 7-MBA-12-CH_2-C8dG. The NMR spectrum of 7-MBA-12-CH_2-C8dG (Figure 2B) and the spectrum after D_2O exchange (Figure 2C) are consistent with the assigned structures. The absence of the sharp singlet at 8.0 ppm assigned to the C-8 proton of the Gua moiety suggests that substitution occurred at this position in dG. The protons 1′-H, 2′-H, 3′-H, 4′-H, and 5′-H_2 in the aliphatic region are unequivocally assigned by COSY. The two broad signals at 4.90 and 5.09 ppm are tentatively assigned as originating from the 5′-OH and 3′-OH, respectively. These two signals disappear with D_2O exchange (Figure 2C), substantiating the assignment of these protons. The aromatic proton resonances, except for 8-H and 11-H, are assigned by using COSY and by comparing their chemical shifts with those of the parent 7,12-DMBA (Figure 3A). The singlet at 3.05 ppm is initially assigned to the 7-CH_3 and the singlet at 5.19 ppm to the 12-CH_2. In the NOE experiment, irradiation of the resonance at 5.19 ppm enhances the two doublets at 8.59 and 8.29 ppm (data not shown). Similarly, irradiation of the singlet resonance at 3.05 ppm enhances the two doublets at 8.41 and 8.09 ppm. Because the two doublets

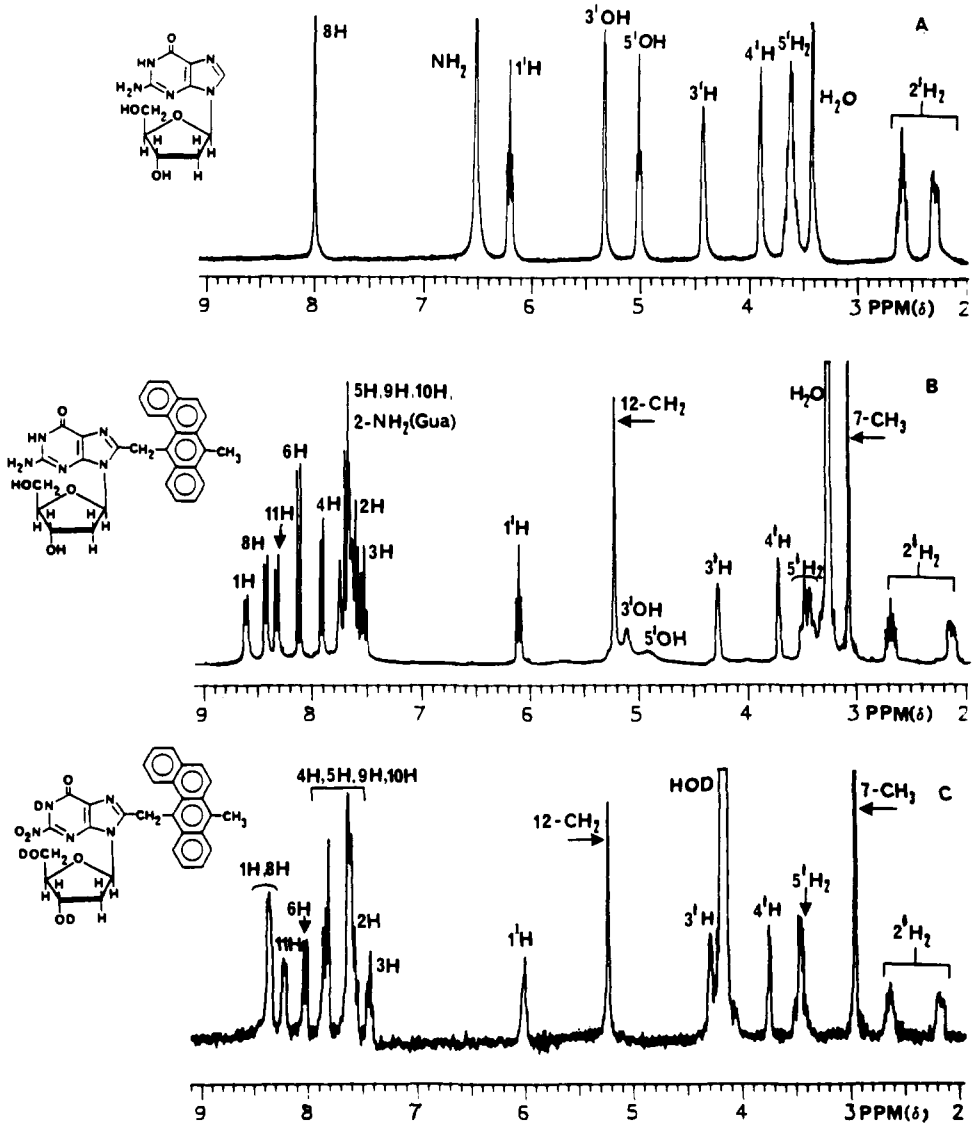

Figure 2. NMR spectra of (A) dG, (B) 7-MBA-12-CH_2-C8dG, and (C) 7-MBA-12-CH_2-C8dG after exchange with D_2O.

at 8.59 and 8.09 ppm are already established as resonances for 1-H and 6-H, the NOE experiments allow us to assign the 8-H and 11-H resonances, respectively, at 8.41 and 8.29 ppm. Furthermore, the covalent bond between dG and the 12-CH_3 group of 7,12-DMBA is unequivocally established.

The resonances of the NH_2 of Gua are thought to be part of the aromatic multiplet at 7.59–7.75 ppm (Figure 2B). This hypothesis is supported by the integration values in the spectrum in Figure 2B vs that obtained after D_2O exchange (Figure 2C). The downfield shift of the NH_2 of the Gua moiety is presumably due to its interaction with the angular ring of the 7,12-DMBA moiety in the region corresponding to 2-H and 3-H, whose resonances are shifted downfield with respect to those of 7,12-DMBA (Figure 3A).

b. 7-MBA-12-CH_2-C8Gua. The NMR spectrum of 7-MBA-12-CH_2-C8Gua (Figure 3B) resembles that of 7-MBA-12-CH_2-C8dG, except for the absence of the proton signals from the deoxyribose moiety. Assignment of protons is obtained by comparison of the chemical shifts with those of the parent compound, 7,12-DMBA, and by COSY. The bond between 7,12-DMBA and Gua is definitively established by NOE experiments in which the protons at 3.14 ppm, corresponding to 7-CH_3, and 5.21 ppm, corresponding to 12-CH_2, are irradiated. The broad singlet at 6.73 ppm is assigned as due to the 7- or 9-NH of Gua, as determined by their disappearance after exchange with D_2O (figure not shown). The NH_2 protons of Gua are deshielded in the region of the aromatic protons at 7.59–7.80 ppm, as seen for 7-MBA-12-CH_2-C8dG in Figure 2B. The D_2O exchange and integration data support this assignment.

c. 7-MBA-12-CH_2-N7Gua. The NMR spectrum (Figure 3C) of 7-MBA-12-CH_2-N7Gua contains a sharp singlet at 8.26 ppm of the C-8 proton of Gua, indicating that this position is not substituted. In addition, the signal at 7.20 ppm, corresponding to the two protons of the NH_2 of Gua, is evidence that no substitution occurred at the amino group. Furthermore, this molecule does not contain the deoxyribose moiety because the corresponding proton resonances in the aliphatic region are absent. This is consistent with substitution of dG at N-7, which destabilizes the glycosidic bond.

The covalent bond of the 7,12-DMBA moiety at the 12-CH_2 is assigned from NOE experiments. This is further substantiated by the shift upfield of the resonances for 1-H and 11-H, appearing at 7.91–8.04 ppm. The remaining protons of 7,12-DMBA are assigned by comparing their chemical shifts with those of the parent compound, 7,12-DMBA, and by using COSY.

d. 12-MBA-7-CH_2-N7Gua. The bonding site for 12-MBA-7-CH_2-N7Gua was assigned from the NOE difference spectrum after irradiation of the singlet at 5.36 ppm, which resulted in enhancement of the two doublets at 8.11 and 8.31 ppm (Figure 3D). The doublet at 8.11 ppm is established for the 6-H. Hence, the other doublet involved in the NOE experiment is assigned to 8-H, establishing that this compound is a 7-CH_2-Gua adduct. Other aromatic signal assignments were easily made by using COSY and by comparing with the NMR of the parent compound,

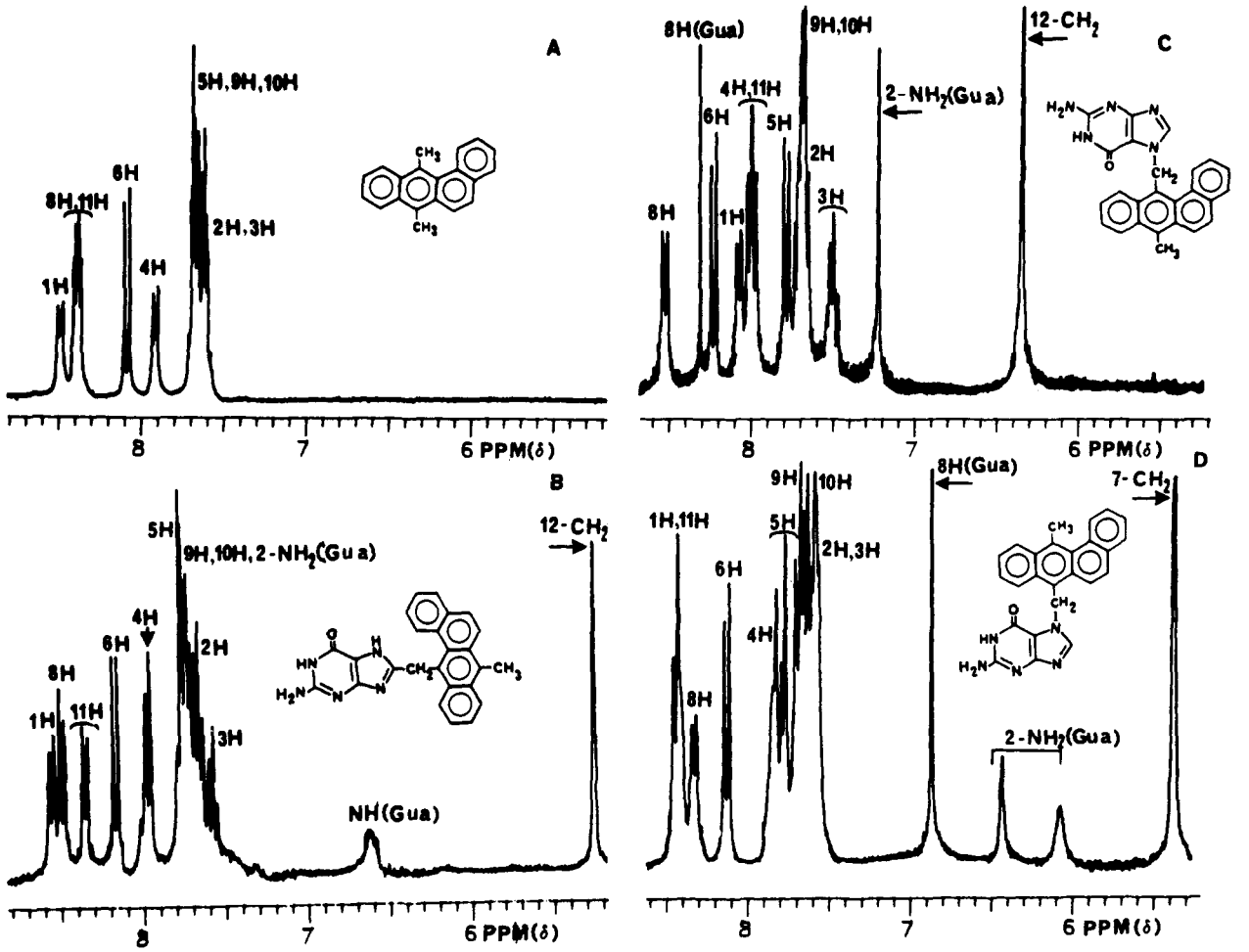

Figure 3. NMR spectra of (A) 7,12-DMBA, (B) 7-MBA-12-CH_2-C8Gua, (C) 7-MBA-12-CH_2-N7Gua, and (D) 12-MBA-7-CH_2-N7Gua.

7,12-DMBA. The broad singlets at 6.41 and 6.09 ppm disappear on D_2O exchange. Thus, these two are assigned to the 2-NH_2 of Gua. The sharp singlet at 6.85 ppm is tentatively assigned as arising from the 8-H of Gua. This is consistent with substitution of the Gua moiety at N-7 by the 7-CH_2 of 7,12-DMBA. The strong shielding effects of the 8-H of Gua and one of the NH_2 protons can be attributed to electronic perturbation of the aromatic rings of 7,12-DMBA.

e. 7,12-$(CH_2OH)_2$-BA. The NMR spectrum (figure not shown) of the dihydroxy compound is fairly simple, and the aromatic region resembles very much that for 7,12-DMBA, except that the signal for 11-H is shifted upfield by 0.15 ppm. COSY allows us to assign all of the resonance frequencies. The two singlets at 5.30 and 5.45 ppm are assigned to 7-CH_2 and 12-CH_2, respectively.

f. 7-MBA-12-CH_2-N7Ade. This molecule does not have the deoxyribose moiety because the corresponding proton resonances in the NMR spectrum (Figure 4A) are absent. The broad singlet at 7.16 ppm, which disappears after D_2O exchange, is established as the resonances of the two protons of NH_2 of Ade, demonstrating that no substitution occurs at the amino group. The COSY spectrum allows us to assign all of the protons, except for those giving the two doublets at 7.80 and 8.50 ppm and that yielding the multiplet at 8.00 ppm. The sharp singlet at 8.29 ppm is designated as arising from 2-H of Ade by comparison of its chemical shift with that of the corresponding proton in dA (spectrum not shown). The other sharp singlet, at 7.70 ppm, is tentatively assigned to the 8-H of Ade. This proton resonance is at 8.2 ppm in dA. Thus, the shift upfield suggests that the PAH is linked to Ade at the N-7; a similar shift was observed in Figure 3D for 12-MBA-7-CH_2-N7Gua. The singlet at 3.17 ppm is initially assigned to 7-CH_3 and the singlet at 6.46 ppm to 12-CH_2.

To confirm many of the assignments postulated above, NOE experiments were conducted by irradiating the two singlet resonances corresponding to 12-CH_2 and 7-CH_3 at 6.46 and 3.17 ppm, respectively. In the NOE experiment, irradiation of the singlet resonance at 3.17 ppm enhances the intensity of the two doublets at 8.23 and 8.54 ppm. Because the doublet at 8.23 ppm is already assigned by COSY to 6-H, the other doublet can be assigned to 8-H, and the singlet at 3.17 ppm is confirmed to be due to 7-CH_3. When the singlet resonance at 6.46 ppm is irradiated, an NOE is observed in which the doublets at 7.80 and 8.00 ppm, the sharp singlet at 7.70 ppm, and the broad singlet at 7.16 ppm are enhanced (Figure 4B). This is expected when the 12-CH_2 is covalently bound to N-7 of Ade, because the protons 1-H and 11-H of 7,12-DMBA and the 6-NH_2 and 8-H of Ade are in the vicinity of the 12-CH_2 of 7,12-DMBA. Thus, the NOE experiment unequivocally establishes the bond between the N-7 of Ade and the 12-CH_2 of 7,12-DMBA.

g. 12-MBA-7-CH_2-N3Ade. The NMR spectrum (Figure 4C) clearly shows the absence of deoxyribose. The presence of the two prominent singlets at 6.98 and 8.24 ppm, initially assigned as the resonances of 2-H and 8-H of Ade, indicates that these positions are not substituted. In addition, the two protons that give a resonance at 7.27 ppm are established as the 6-NH_2 of Ade, demonstrating that no substitution occurs at the amino group. The chemical shifts and proton multiplicities of this spectrum do not correspond to those of the NMR of the N7-Ade adduct (Figure 4A), demonstrating that this is not an N-7 adduct. Because N-3 is a nucleophilic group of Ade and a covalent bond to this position would destabilize the glycosidic bond of deoxyribose, it is logical to hypothesize that adduction occurred at N-3. This is further substantiated by the large upfield shift, 1.3 ppm, of the 2-H proton resonance.

Once again NOE experiments unequivocally prove the structure of the adduct. The NOE spectrum (Figure 4D) obtained from irradiation of the singlet resonance at 6.52 ppm shows enhancement of the 6-H and 8-H doublets at 8.02 and 8.29 ppm, re-

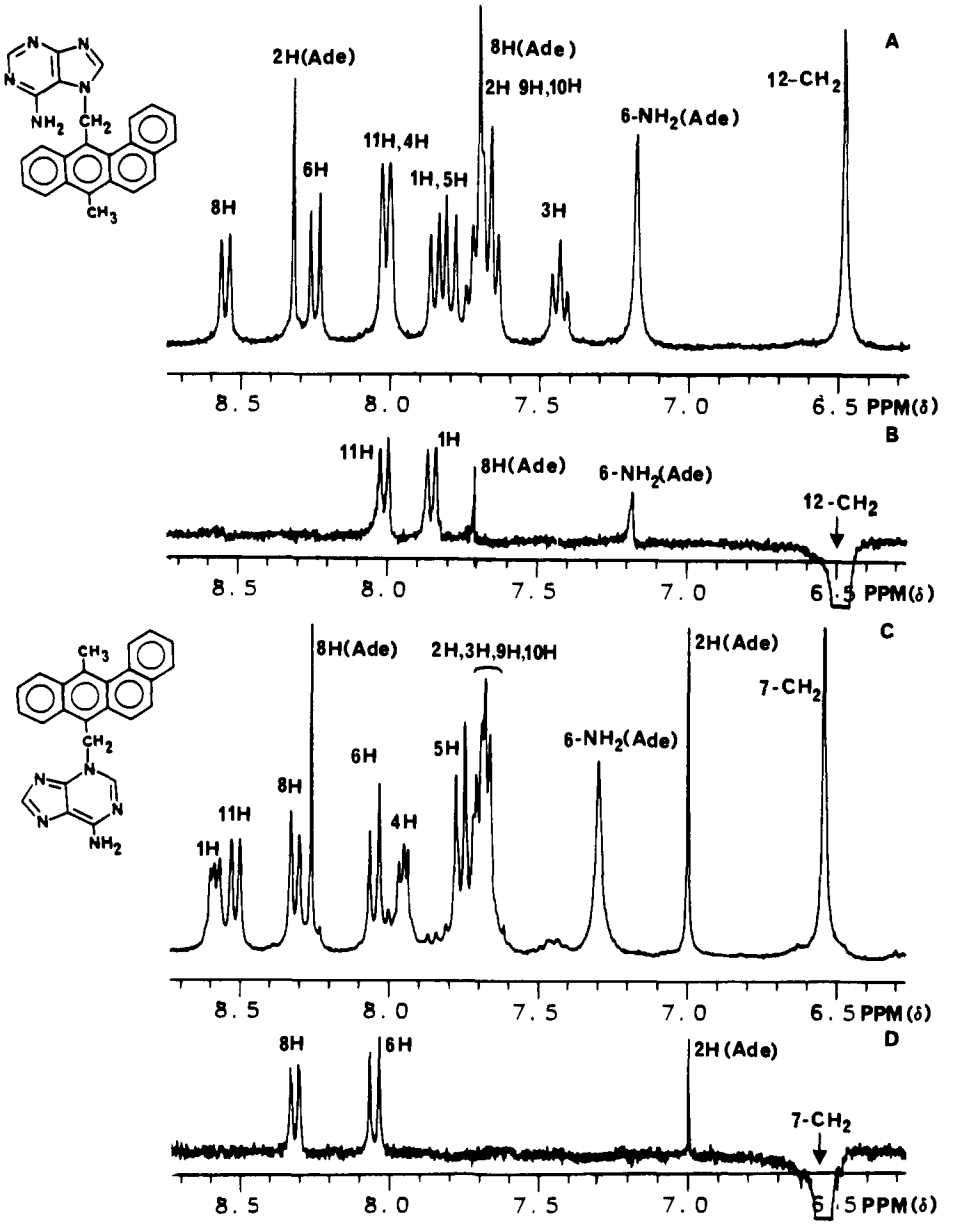

Figure 4. (A) NMR spectrum of 7-MBA-12-CH_2-N7Ade. (B) NOE spectrum of 7-MBA-12-CH_2-N7Ade after irradiation at 6.46 ppm (corresponding to 12-CH_2). (C) NMR spectrum of 12-MBA-7-CH_2-N3Ade. (D) NOE spectrum of 12-MBA-7-CH_2-N3Ade after irradiation at 6.52 ppm (corresponding to 7-CH_2).

spectively, and the sharp singlet at 6.98 ppm, corresponding to the 2-H of Ade (Figure 4D). The enhancement of the two doublets unequivocally indicates that the 7-CH_2 of 7,12-DMBA is the position of linkage in the adduct, and the singlet at 3.39 ppm corresponds to a resonance for the 12-CH_3. The enhancement of the signal of the 2-H of Ade is proof that the N-3 of Ade is bound to 7,12-DMBA. On the other hand, the absence of enhancement of the NH_2 signal in the NOE experiment clearly establishes that this adduct does not involve binding at N-7 of Ade; this is in contrast to the enhancement observed in Figure 4B for the N7-Ade adduct. The remaining protons in the aromatic region are designated by comparing their chemical shifts with those of the parent compound, 7,12-DMBA, and by employing COSY.

Structure Elucidation by FAB MS/MS. a. 7-MBA-12-CH_2-C8dG. FAB of 7-MBA-12-CH_2-C8dG produces an $(M + H)^+$ ion of m/z 522 (observed 522.2130; theoretical for $C_{30}H_{28}N_5O_4$ 522.2141). Upon collisional activation, the $(M + H)^+$ ion fragments to produce six ions that are diagnostic of the structure of the adduct. Two ions indicate the presence of the sugar: the ion of m/z 405 results from the loss of the intact sugar from $(M + H)^+$, and the ion of m/z 432 results from an extrusion of $C_3H_6O_3$ from the sugar moiety, as was previously observed.[45] Two other ions indicate the presence of Gua: the m/z 152 ion is protonated Gua, and the m/z 164 ion is $(Gua - H + CH_2)^+$ ion, indicating the attachment of Gua to one of the CH_3 groups of the 7,12-DMBA. The presence of 7,12-DMBA is also indicated by three ions: the ion of m/z 255, which is identical in mass to the $(M - H)^+$ ion of 7,12-DMBA, results from the cleavage of the PAH–nucleoside bond, and the ions of m/z 239 and 240 result from losses of CH_4 and CH_3 from the m/z 255 ion.

Preliminary studies on the ability of tandem MS to determine the structure of 7,12-DMBA adducts were conducted on adducts formed with pyridine.[46] This previous investigation indicates that one can distinguish the position of pyridine attachment to 7,12-DMBA because the structure of the m/z 255 ion (presumably a fused-ring tropylium ion) is dependent on the position of the leaving group. This should remain true if the leaving group is changed from a pyridine to a nucleoside moiety. In fact, the position of Gua, dG, or Ade attachment to 7,12-DMBA was

(45) Crow, F. W.; Tomer, K. B.; Gross, M. L.; McCloskey, J. A.; Bergstrom, D. E. *Anal. Biochem.* **1984**, *139*, 243–262.
(46) Dolnikowski, G. G.; Cavalieri, E. L.; Gross, M. L. *J. Am. Soc. Mass Spectrom.* **1991**, *2*, 256–258.

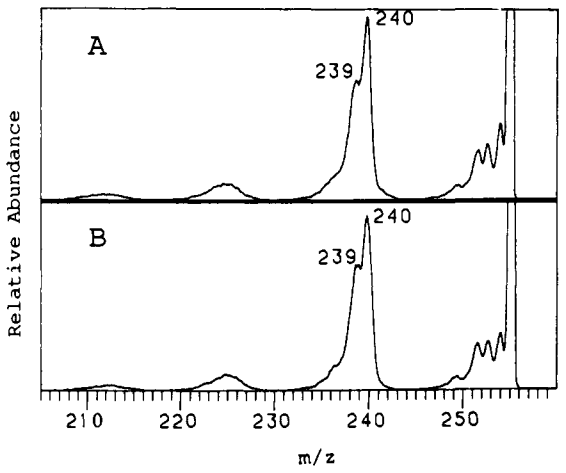

Figure 5. (A) Partial CAD spectrum of m/z 255 fragment ion from 7-MBA-12-CH_2-C8dG. (B) Partial CAD spectrum of m/z 255 fragment ion from 7-MBA-12-CH_2-pyridinium salt.

determined by comparing the CAD product ion spectrum of the m/z 255 ion produced by FAB of the DNA adducts to those of the m/z 255 ions produced from a series of 7,12-DMBA-pyridinium adducts of known structure.[46] The CAD spectrum of the source-produced ions of m/z 255 from 7-MBA-12-CH_2-C8dG (Figure 5A) shows that an abundant ion of m/z 240 and a slightly less abundant ion of m/z 239 are formed, just as does the CAD spectrum of the m/z 255 ion produced upon FAB from a 7-MBA-12-CH_2-pyridinium salt (Figure 5B). This confirms adduct formation at the 12-CH_3 position of 7,12-DMBA.

Whether 7,12-DMBA is attached to the C-8 or N-7 position of the Gua is more difficult to determine on the basis of the CAD spectra. We expect that a C–C adduct bond should be slightly stronger than a C–N adduct bond, so the CH_2-N7 adduct should fragment more readily than the CH_2-C8 adduct and, therefore, give more abundant m/z 255 ions. This is indeed the case: the $(M + H)^+/(M + H - Gua)^+$ abundance ratio is on average 40 in the two cases where NMR indicated CH_2–C8 linkages and is on average 32 in the two cases where NMR indicated a CH_2–N7 linkage. These ratios vary somewhat with collision cell conditions, but under constant conditions of collision cell pressure, the CH_2-C8 adducts always have higher $(M + H)^+/(M + H - Gua)^+$ abundance ratios than do the CH_2-N7 adducts. This distinction requires that reference adducts be studied in parallel with sample adducts. FLNS gives a clearer distinction, as is discussed later in this paper.

b. 7-MBA-12-CH_2-C8Gua. FAB of 7-MBA-12-CH_2-C8Gua gives an $(M + H)^+$ ion of m/z 406 (observed 406.1670; theoretical for $C_{25}H_{20}N_5O^+$ is 406.1667). The CAD spectrum of the m/z 406 ion shows that four major fragments are formed. The ion of m/z 255, which is identical in mass to the $(M - H)^+$ of 7,12-DMBA, indicates the loss of Gua from the protonated adduct. The ion of m/z 239 is due to CH_4 loss from the m/z 255 ion. Ions of m/z 152 and 164 are protonated Gua and $(Gua - H + CH_2)^+$, respectively. The CAD spectrum of the m/z 255 fragment ion is nearly identical to those of the m/z 255 ions from 7-MBA-12-CH_2-C8dG and 7-MBA-12-CH_2-pyridinium ion,[46] indicating Gua is attached to the 12-CH_3 group of the 7,12-DMBA.

c. 7-MBA-12-CH_2-N7Gua. FAB of 7-MBA-12-CH_2-N7Gua also produces an $(M + H)^+$ ion of m/z 406 (observed 406.1668; theoretical for $C_{25}H_{20}N_5O^+$ is 406.1667). Collisional activation (CA) of the m/z 406 ion yields the same major product ions as does CA of the $(M + H)^+$ of 7-MBA-12-CH_2-C8Gua. Furthermore, the CAD spectrum of the m/z 255 ion is again nearly identical to that of the m/z 255 ion from the 7-MBA-12-CH_2-pyridinium ion,[46] confirming that Gua is attached to the 12-CH_3 group of the 7,12-DMBA.

d. 12-MBA-7-CH_2-N7Gua. FAB of 12-MBA-7-CH_2-N7Gua gives an $(M + H)^+$ ion of m/z 406 (observed 406.1665; theoretical for $C_{25}H_{20}N_5O^+$ is 406.1667). The CAD spectrum of the m/z 406 ion shows that fragment ions of m/z 255, 152, and 164 are formed, consistent with the CAD spectra of adducts discussed previously. There is, however, one difference with respect to that of 7-MBA-12-CH_2-N7Gua: the ion of m/z 239 is more abundant than that of m/z 240. Likewise, the CAD spectrum of the m/z 255 fragment ion produced in the ion source upon FAB displays similar properties; that is, the ion of m/z 239 is again of greater abundance. This is consistent with the CAD spectrum of the m/z 255 ion from the 12-MBA-7-CH_2-pyridinium ion[46] and is distinctive evidence that Gua is attached to the 7-CH_3 group of the 7,12-DMBA.

e. 7-MBA-12-CH_2-N7Ade and 12-MBA-7-CH_2-N3Ade. FAB of 7-MBA-12-CH_2-N7Ade produces an $(M + H)^+$ ion of m/z 390 (observed 390.1720; theoretical for $C_{25}H_{20}N_5^+$ is 390.1719) as does FAB of 12-MBA-7-CH_2-N3Ade (observed 390.1721). The CAD spectra of the $(M + H)^+$ species are indistinguishable, but the isomers can be distinguished by MS/MS studies of the m/z 255 fragment ion, which corresponds to $(M - H)^+$ of 7,12-DMBA. Because the three-sector tandem instrument has only an electrostatic analyzer with a mass resolution of ca. 150 for the second stage, the differences in the abundances of ions of m/z 239 and 240 were difficult to recognize, especially in the CAD spectra of the modified nucleoside $(M + H)^+$ ion.

Recently, a new four-sector mass spectrometer, the prototype VG Analytical ZAB-T, was installed at the University of Nebraska—Lincoln. This instrument is double-focusing for both MS-I and MS-II, resulting in improved resolution of MS-II. CAD spectra of the nucleoside $(M + H)^+$ ions of m/z 390 for 12-MBA-7-CH_2-N3Ade (Figure 6A) and 7-MBA-12-CH_2-N7Ade (Figure 6B) were obtained with this new four-sector instrument. Common features in both spectra are the ions of m/z 255 $(7,12\text{-DMBA} - H)^+$, m/z 136 (protonated Ade), and m/z 148 $(Ade + CH_2)^+$. These ions are analogous to those observed in the CAD spectra of the 7,12-DMBA-Gua adducts. Differences in the relative abundances of m/z 239 and 240 ions can be readily seen without turning to activation of the m/z 255 ions (see inserts). The larger relative abundance of m/z 239 in Figure 6A indicates adduct formation at the 7-CH_3 position of 7,12-DMBA; the more abundant m/z 240 in Figure 6B identifies the 12-CH_3 as the site of bonding. These differences in relative abundances are also consistent with those observed in the CAD spectra obtained with the three-sector tandem for the m/z 255 fragment ion of pyridinium-7,12-DMBA adducts.[46]

Analysis of Adducts by FLNS. FLNS can be used to distinguish between nucleoside adduction at the 7-CH_3 and 12-CH_3 groups of 7,12-DMBA and, furthermore, to determine whether attachment of 7,12-DMBA occurs at the C-8 or N-7 positions of Gua and to the N-7 or N-3 positions of Ade. All of the 7,12-DMBA-nucleoside adducts studied aggregate in the glass solvent at room temperature, as well as in the glass at low temperatures. Although oligomer formation at room temperature can be eliminated by dilution, it was found that oligomers persisted in the glass for concentrations as low as 10^{-8} M. Apparently, the stabilization energy of n-solvated monomers is less than that of a solvated oligomer of n-monomers near the glass transition temperature.[47]

The oligomer fluorescence for all adducts is substantially red-shifted and very broad relative to that of the monomer. For all adducts, the fluorescence origin bands for the monomer and oligomers are at ca. 400 and ca. 405 nm, respectively, and, thus, some spectral discrimination is possible. In addition, the oligomer fluorescence lifetime is considerably shorter than the monomer fluorescence lifetime of ca. 130 ns. For this reason, a 50–150-ns observation window was employed to reduce further the interference from the oligomer fluorescence to the structured FLN spectra of the monomer. Only the most highly resolved FLN spectra of the electrochemically synthesized 7,12-DMBA adducts are presented here. These standard FLN spectra are essential for future in vitro and in vivo studies of 7,12-DMBA adducts formed by the one-electron oxidation pathway.

(47) Martinaud, M.; Kottis, P. *J. Phys. Chem.* **1978**, *82*, 1497–1505.

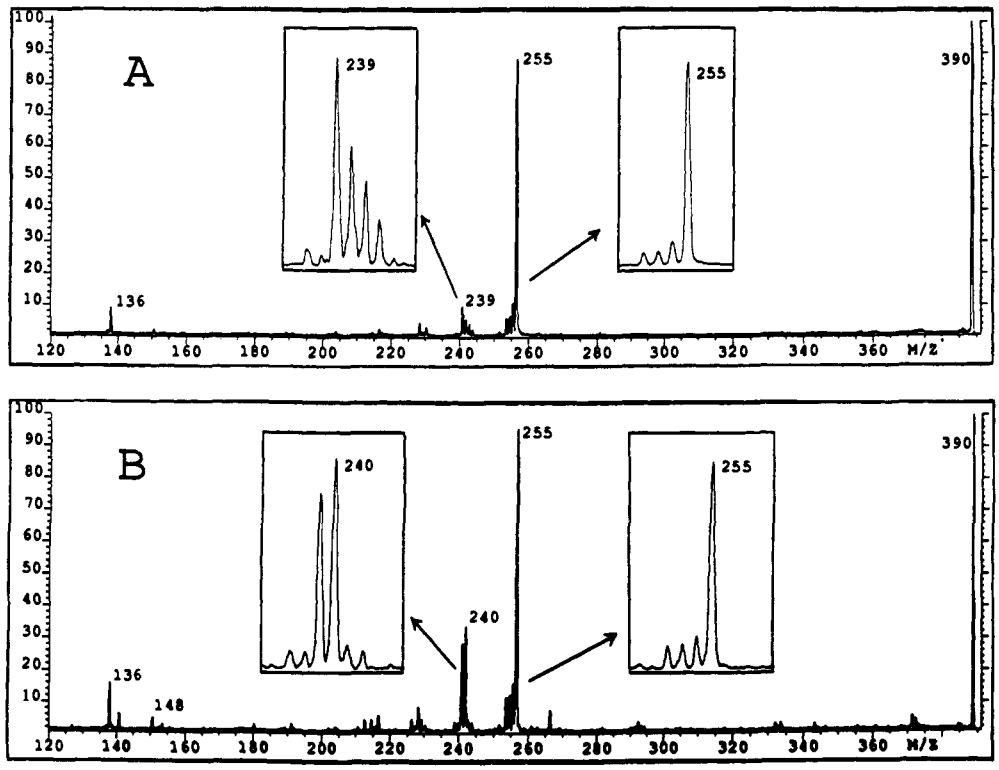

Figure 6. (A) CAD spectrum of $(M + H)^+$ of 12-MBA-7-CH_2-N3Ade. (B) CAD spectrum of $(M + H)^+$ of 7-MBA-12-CH_2-N7Ade. Inserts are magnifications of the definitive fragment ion regions.

Table I. Excited-State (S_1) Vibrational Frequencies (cm^{-1}) of 7,12-DMBA and Its Adducts Formed with dG and dA by Electrochemical Oxidation

7,12-DMBA	7-MBA-12-CH_2-C8dG	7-MBA-12-CH_2-C8Gua	7-MBA-12-CH_2-N7Gua	12-MBA-7-CH_2-N7Gua	7-MBA-12-CH_2-N7Ade	12-MBA-7-CH_2-N3Ade
	220	220	220	221	221	221
267	271	270	273	267	273	267
321	311	310	311	309	311	310
373	347	343	355	w[a]	360	355
393	w	w	w	w	398	w
446	421	420	420	408	426	409
486	477	475	482	474	478	472
515	513	511	511	502	510	499
591	538	538	538	538	537	w
631	636	632	636	634	634	638
662					710	

[a] w, weak.

A segment of the FLN spectra of 12-MBA-7-CH_2-N7Gua (spectrum A) and of 7-MBA-12-CH_2-N7Gua (spectrum B) is presented in Figure 7. These spectra of the vibronically excited species were obtained with λ_{ex} = 390 nm. The line-narrowed bands for both adducts (monomer), which are labeled according to their excited state (S_1) vibrational frequencies in cm^{-1}, are superimposed on the high-energy tail of the broad oligomer fluorescence discussed above. Although the FLN spectra of 12-MBA-7-CH_2-N7Gua and 7-MBA-12-CH_2-N7Gua are quite similar, significant differences in vibrational frequencies are observed (e.g., 408, 474, and 502 cm^{-1} for the former vs 420, 482, and 511 cm^{-1} for the latter). More complete listings of vibrational frequencies obtained from Figure 7 and other FLN spectra are given as the fifth and fourth columns of Table I. For comparison, the corresponding frequencies for 7,12-DMBA are given in the first column.

The spectra of Figure 7 and others obtained with different λ_{ex} values indicate the S_1 state of 7-MBA-12-CH_2-N7Gua lies about 100 cm^{-1} lower in energy than that of 12-MBA-7-CH_2-N7Gua. This explains why the vibronic intensity distributions of spectra A and B of Figure 7 are significantly different (e.g., note that the 636-cm^{-1} signal is considerably more intense in spectrum B than in spectrum A). Thus, these two N7Gua adducts can be distinguished on the basis of vibronic frequencies and the intensity

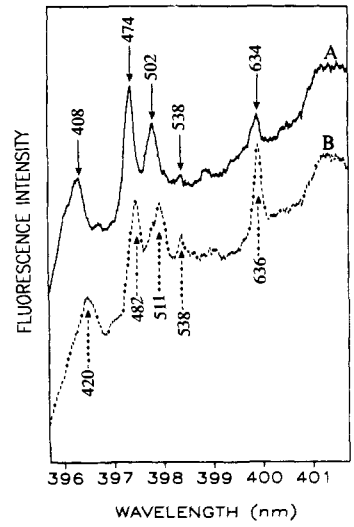

Figure 7. Vibronically excited FLN spectra of 12-MBA-7-CH_2-N7Gua (A) and 7-MBA-12-CH_2-N7Gua (B) obtained at T = 4.2 K with λ_{ex} = 390 nm.

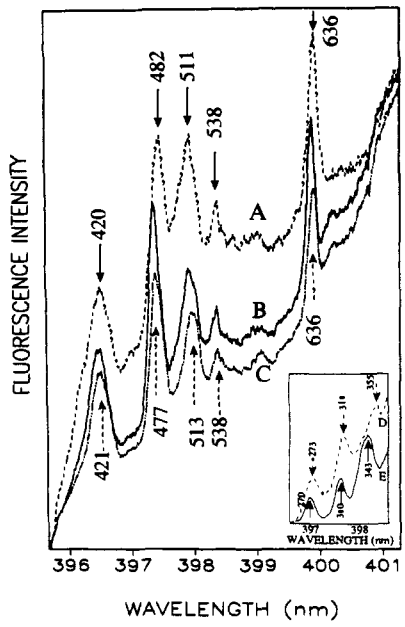

Figure 8. FLN spectra of 7-MBA-12-CH_2-N7Gua (A and D), 7-MBA-12-CH_2-C8Gua (B and E), and 7-MBA-12-CH_2-C8dG (C) obtained at T = 4.2 K with λ_{ex} = 390 nm.

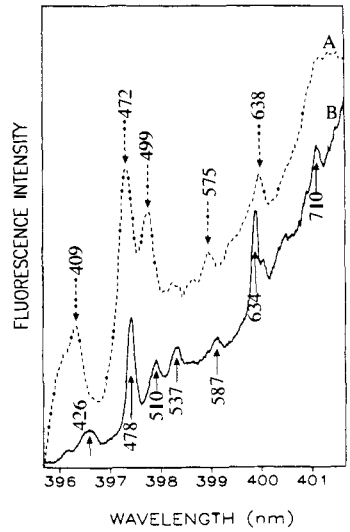

Figure 9. FLN spectra of 12-MBA-7-CH_2-N3Ade (A) and 7-MBA-12-CH_2-N7Ade (B) obtained at T = 4.2 K with λ_{ex} = 390 nm.

distribution. This is only possible for a binary mixture when the concentrations of the two adducts are comparable.

The FLN spectra for the 7-MBA-12-CH_2-N7Gua, 7-MBA-12-CH_2-C8Gua, and 7-MBA-12-CH_2-C8dG adducts obtained with λ_{ex} = 390 nm are shown in Figure 8, spectra A–C, respectively. Portions of the FLN spectra for the former two adducts obtained with λ_{ex} = 392.8 nm are shown in the inset to this figure. Comparison of the spectra for 7-MBA-12-CH_2-N7Gua and 7-MBA-12-CH_2-C8Gua reveals that these two adducts can be distinguished on the basis of the FLN spectral shifts of the 355- (Figure 8D) and 482-cm^{-1} (Figure 8A) modes of the former adduct to 343 (Figure 8E) and 477 cm^{-1} (Figure 8B) for 7-MBA-12-CH_2-C8Gua. The 7-MBA-12-CH_2-C8Gua (Figure 8B) cannot, however, be differentiated from 7-MBA-12-CH_2-C8dG (Figure 8C). This is also the case for the C8Gua and C8dG one-electron oxidation adducts of benzo[*a*]pyrene.[42] The vibrational frequencies for 7-MBA-12-CH_2-C8Gua are listed in Table I, column 3.

The FLN spectra for the 12-MBA-7-CH_2-N3Ade and 7-MBA-12-CH_2-N7Ade adducts are compared in Figure 9, spectra A and B, respectively. The vibrational mode frequencies for these two adducts are strikingly different, as are the vibronic intensity

Scheme II. One- and Two-Electron Oxidation of 7,12-DMBA To Form Benzylic Radical Intermediates and Benzylic Carbenium Ion Intermediates, Respectively

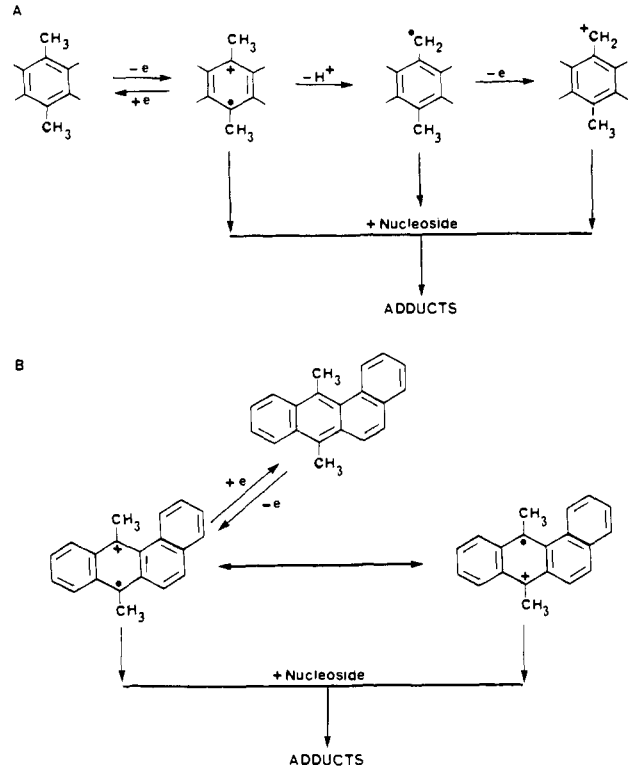

distributions. Thus, their differentiation by FLNS is straightforward. Their vibrational frequencies are given in the last two columns of Table I. Therefore, all of the adducts formed can be distinguished by FLNS.

Mechanism of Adduct Formation. Electrochemical oxidation of 7,12-DMBA in the presence of dG or dA not only provides standard adducts that can be formed in biological systems but also offers information on the specific reactivity of the CH_3 groups of 7,12-DMBA and the nucleophilic sites on the purine bases. In fact, upon oxidation 7,12-DMBA reacts predominantly at the 12-CH_3 group and aralkylation occurs specifically at the N-7 and C-8 nucleophilic groups of Gua. For Ade the N-7 covalently binds at the 12-CH_3, whereas the N-3 attaches to the 7-CH_3 of 7,12-DMBA.

Reaction of nucleophilic groups of dA or dG can occur with a radical cation intermediate, a benzylic radical, or a benzylic carbenium ion (Scheme IIA). Anodic oxidation of 7,12-DMBA requires removal of two electrons to form adducts. For the radical cation and benzylic radical, the second electron is apparently removed after coupling with the nucleoside (not shown), whereas formation of the benzylic carbenium ion requires that the two electrons be removed sequentially from the 7,12-DMBA. In fact, redox of 7,12-DMBA by cyclic voltammetry under reversible conditions involves one electron.

The critical intermediate for the adduction is not a benzylic-type carbenium ion because, as reported in this paper, the distribution of adduct isomers obtained electrochemically from 7,12-DMBA with dG in DMF is very different from that obtained by reaction of 12-MBA-7-CH_2Br with dG in DMF. In this latter reaction, in which a carbenium ion is the intermediate, the two products obtained in approximately equal amounts are the exocyclic amino-substituted product, N^2dG adduct, and the N7Gua adduct. When 7-MBA-12-CH_2OAc or 7-MBA-12-CH_2Br reacts in DMF at 140 °C in the presence of dG, the only product obtained is the N^2Gua adduct. Under these drastic conditions, the sugar moiety is lost. These results are consistent with those obtained from the reaction of 7-CH_2BrBA and 12-MBA-7-CH_2Br with dG in aqueous solvent, in which the major adduct is always the N^2dG adduct.[48-50] When an aprotic solvent such as DMF or di-

methylacetamide is added, increasing amounts of the N7Gua adduct are obtained.[45,48]

Electrochemical oxidation of 7,12-DMBA never yields any trace of N^2dG aralkylation but does give adducts involving the N-7 of Gua and the C-8 of dG. In contrast, the C8dG adduct is never obtained from benzylic carbenium ion intermediates, as reported here and in the literature.[48-51] These data tend to exclude a carbenium ion intermediate in the electrochemical oxidation.

Reaction to form an adduct can also occur between the 12-benzylic radical produced by loss of a proton from the radical cation (Scheme IIA) and, for example, the C-8 position of dG. The rate of adduct formation in anodic oxidation of 7,12-DMBA and dG, however, is not affected by the presence of 2,6-di-*tert*-butylpyridine, which is a base but not a nucleophile, suggesting that the benzylic radical is not formed as a discrete intermediate.

Therefore, we favor reaction between the N-7 and C-8 of the Gua moiety and the 7- or 12-CH_3 group of the 7,12-DMBA radical cation (Scheme IIB). At the present time, mechanistic details of this reaction are not established.

Electrochemical oxidation of 7,12-DMBA also produces N-7 and N-3 adducts of Ade at the 12-CH_3 and 7-CH_3, respectively. In contrast, reaction of adenosine with 7-CH_2BrBA or other benzylating agents produces the N-1 and exocyclic amino-substituted N^6 adducts but not the N-7 and N-3 adducts.[48,51] Thus, it is logical to assume that the same radical cation intermediate described above for reaction with dG operates in the adduction to dA.

Covalent binding of 7,12-DMBA to DNA by horseradish peroxidase-catalyzed and cytochrome P-450-catalyzed one-electron oxidation yields 7-MBA-12-CH_2-N7Gua and 7-MBA-12-CH_2-N7Ade, whereas 12-MBA-7-CH_2-N7Gua and 12-MBA-7-CH_2-N3Ade are not formed.[52] This study provides additional evidence that these two adducts are obtained via a radical cation intermediate, forging a link between the electrochemical and enzymatic experiments. Furthermore, the 12-CH_3 group is critical in the binding of the 7,12-DMBA to the nucleophiles of DNA in biological systems.

Conclusions

The radical cation of 7,12-DMBA reacts with dG to produce 7-MBA-12-CH_2-C8dG, 7-MBA-12-CH_2-N7Gua, and 12-MBA-7-CH_2-N7Gua. The 7-MBA-12-CH_2-C8Gua is a secondary product arising from electrochemical oxidation of the corresponding C8dG adduct, whereas 7,12-$(CH_2OH)_2$-BA is formed by electrochemical oxidation of 12-MBA-7-CH_2-N7Gua to form an N7Gua diadduct, which is rapidly hydrolyzed to 7,12-$(CH_2OH)_2$-BA during HPLC. With dA, the two adducts formed, in approximately equal amounts, are 7-MBA-12-CH_2-N7Ade and 12-MBA-7-CH_2-N3Ade. No detectable adducts are formed with dC or T. The synthesis is not only a demonstration of the reactivity of nucleosides and 7,12-DMBA under oxidizing conditions but also a source for necessary reference materials for studying the 7,12-DMBA-DNA adducts formed in biological systems.

Of particular importance to future biological studies is the ability of FAB MS/MS, as well as FLNS, to distinguish between the adducts of 7,12-DMBA at the 7- and 12-CH_3 groups and the N-7 and C-8 positions of Gua. FLNS also possesses the necessary selectivity to distinguish between 12-MBA-7-CH_2-N3Ade and 7-MBA-12-CH_2-N7Ade. On the other hand, the distinction between 7-MBA-12-CH_2-C8Gua and 7-MBA-12-CH_2-C8dG is straightforward by FAB MS/MS but very difficult by FLNS. Thus, the two techniques complement each other very nicely.

A mechanism of adduction is proposed in which a radical cation is formed by anodic oxidation and reacts via the methyl groups with various nucleophilic groups of dA and dG.

Acknowledgment. We thank Dr. D. L. Nagel for his advice on the use of the NOE technique in analysis of adduct structures by NMR. This research was primarily supported by USPHS Grant PO1 CA49210, awarded to the three research groups. In addition, the following sources also supported this research: USPHS Grant RO1 CA44686 and core support to the Eppley Institute from the National Cancer Institute (P30-CA36727) and the American Cancer Society (SIG-16). Ames Laboratory is operated for the U.S. Department of Energy by Iowa State University under Contract W-7405-Eng-82, and research at the Ames Laboratory was also supported by the Office of Health and Environmental Research, Office of Energy Research. The mass spectrometry experiments were also supported by National Science Foundation Grant CHE-8620177.

(48) Dipple, A.; Brookes, P.; Mackintosh, D. S.; Rayman, M. P. *Biochemistry* **1971**, *10*, 4323-4330.
(49) Rayman, M. P.; Dipple, A. *Biochemistry* **1973**, *12*, 1202-1207.
(50) Pei, G. K.; Moschel, R. C. *Chem. Res. Toxicol.* **1990**, *3*, 292-295.
(51) Moschel, R. C.; Hudgins, W. R.; Dipple, A. *J. Org. Chem.* **1979**, *44*, 3324-3328.
(52) RamaKrishna, N. V. S.; Devanesan, P. D.; Rogan, E. G.; Cavalieri, E. L.; Jeong, H.; Jankowiak, R.; Small, G. J. *Chem. Res. Toxicol.* **1992**, in press.

Communications to the Editor

Control of Chemoselectivity in Catalytic Carbenoid Reactions. Dirhodium(II) Ligand Effects on Relative Reactivities

Albert Padwa,* David J. Austin, Susan F. Hornbuckle, and Mark A. Semones

Department of Chemistry, Emory University Atlanta, Georgia 30322

Michael P. Doyle* and Marina N. Protopopova

Department of Chemistry, Trinity University San Antonio, Texas 78212

Received October 30, 1991

Rhodium(II) acetate has become the catalyst of choice for reactions of diazo compounds that result in a broad selection of metal carbene transformations including cyclopropanation, carbon-hydrogen insertion, ylide generation, and aromatic cycloaddition.[1-4] High product yields and significant regio- and/or stereocontrol can generally be achieved.[5-9] However, there are few examples which permit evaluation of chemoselectivity for these catalytic reactions, and those that have been reported suggest

(1) (a) Doyle, M. P. *Chem. Rev.* **1986**, *86*, 919. (b) Doyle, M. P. *Acc. Chem. Res.* **1986**, *19*, 348.
(2) Maas, G. *Top. Curr. Chem.* **1987**, *137*, 75.
(3) Adams, J.; Spero, D. M. *Tetrahedron* **1991**, *47*, 1765.
(4) Padwa, A.; Hornbuckle, S. F. *Chem. Rev.* **1991**, *91*, 263.
(5) Doyle, M. P.; Pieters, R. J.; Taunton, J.; Pho, H. Q.; Padwa, A.; Hertzog, D. L.; Precedo, L. *J. Org. Chem.* **1991**, *56*, 820.
(6) Doyle, M. P.; Bagheri, V.; Wandless, T. J.; Harn, N. K.; Brinker, D. A.; Eagle, C. T.; Loh, K.-L. *J. Am. Chem. Soc.* **1990**, *112*, 1906.
(7) (a) Adams, J.; Poupart, M.-A.; Grenier, L.; Schaller, C.; Quimet, N.; Frenette, R. *Tetrahedron Lett.* **1989**, *30*, 1749. (b) Adams, J.; Poupart, M.-A.; Grenier, L. *Tetrahedron Lett.* **1989**, *30*, 1753.
(8) (a) Kennedy, M.; McKervey, M. A.; Maguire, A. R.; Tuladhar, S. M.; Twohig, M. F. *J. Chem. Soc., Perkin Trans. 1* **1990**, 1047. (b) Doyle, M. P.; Shanklin, M. S.; Pho, H. Q. *Tetrahedron Lett.* **1988**, *29*, 2639.
(9) Lee, E.; Jung, K. W.; Kim, Y. S. *Tetrahedron Lett.* **1990**, *31*, 1023.

0002-7863/92/1514-1874$03.00/0